pH-dependent surface charging of metal oxides

Etelka Tombácz

Abstract

Aqueous dispersions of metal oxide particles are of great practical interest due to their wide-ranging industrial applications and everyday uses under the conditions required. The latter involves the broad variability of pH and dissolved materials among them electrolytes which have definite role in charge neutralization in the vicinity of particle surface. In this work, the pH-dependent surface charging of metal oxides due to the specific adsorption of H^+/OH^- in the presence of indifferent and specific ions, and other simultaneous processes at solid/water interface such as hydration of surface, dissociation of surface sites, dissolution of solid matrix, then hydrolysis of dissolved ions are discussed. The governing role of solid particles will be showed by means of characteristic examples of aluminum, iron, titanium and zinc oxides, which have significant differences in chemical properties considering e.g., their pH-dependent dissolution and the speciation of dissolved ions.

Etelka Tombácz

Department of Physical Chemistry and Material Science, University of Szeged, H-6720 Szeged, Aradi Vt.1., Hungary

e-mail: tombacz@chem.u-szeged.hu

1 Introduction

Metal oxide particles are of great practical interest, especially those of aluminum, iron, and recently the titanium and zinc oxides due to their UV absorbance and photocatalytic activity mentioning only some novel reasons for their use. Nowadays, the importance of aqueous dispersions increased definitely because of mainly environmental reasoning. Metal oxides are often used as adsorbents, catalyst carriers, etc. even if they are not directly applied; the adsorption is always involved in their aqueous dispersions.

Adsorption refers to the accumulation of any species from one of the continuous phases at interface between two phases. If solid/liquid (S/L) interface is in question, i.e., adsorption of a dissolved material (solute) is studied, the wetting of solid material (adsorbent) by the liquid (medium in which adsorbent is dispersed) and the solubility of solute in the given liquid (here solvent) have to be considered besides adsorption. Simultaneous equilibria of adsorption, wetting and solubility exist between the components (adsorbent, solvent and solute). Competition of solvent and solute molecules for surface sites and also competition of surface and solvation forces for solute molecules are always present in the S/L adsorption systems. Therefore a better understanding of aqueous oxide dispersions requires that all the interactions be characterized in terms of the fundamental physical and chemical properties of components dissolved (solutes) and dispersed (solid) in the medium (solvent), which is water here.

In aqueous solutions, dissolution of electrolytes results in formation of ionic species, and formation of solid-water interface involves hydration and charging of surface. The ionic species accumulate at interface, which is in fact a chemically controlled distribution of charged species governed by the in situ developed electrified interfaces. Chemical contribution of components cannot be neglected in general; simultaneous equilibria exist both in aqueous phase and at surface which mutually influence each other. The probable simultaneous equilibria between the participating components of adsorption from electrolyte solutions have been discussed in a Chapter 1 of book Adsorption: Theory, Modelling, and Analysis edited by J. Tóth some years

ago. It is worth recalling the knowledge relevant to the aqueous dispersions of metal oxides. The interfacial and aqueous processes resulting in the equilibrium distribution of polar and charged species in oxide dispersions are depicted schematically in Fig. 1. An electrified interface develops due to the formation of multitude charged surface sites and the accumulation of counter-charges in order to preserve charge neutrality. In this pa-

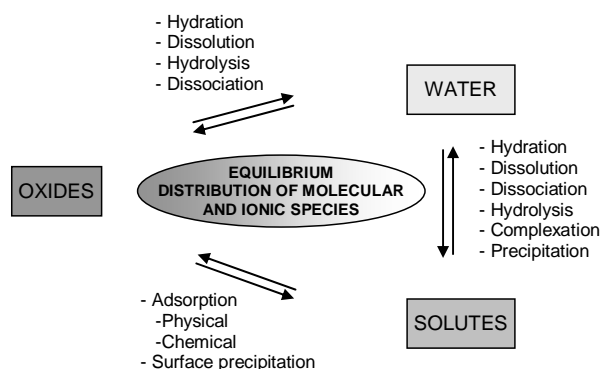SIMULTANEOUS EQUILIBRIA IN AQUEOUS DISPERSIONS OF OXIDES

Fig. 1. Possible solid/water interfacial and aqueous phase processes in metal oxide dispersions

per, I attempt to highlight the importance of simultaneous aqueous and interfacial processes, such as hydration of surface, dissolution of solid, and speciation of dissolved species in aqueous solution phase, which take place in parallel with the adsorption of ionic species and inherently influence the adsorption equilibrium; however, unfortunately, these seem to be often neglected.

2 Theoretical

2.1 Interaction of solid metal oxides with water: hydration, dissolution, hydrolysis and dissociation

The question is how the surface properties of oxide particles alter inherently and charged surface forms during the immersion of solid particles into water. The hydration of solid surfaces starts at solid/gas interface, since it was clearly stated [2] that even under common room conditions (relative humidity in the region 40-60%) two or three layers of adsorbed water are often present on particles, dominating the interactions, and therefore the physical characteristics of the material.

In the case of oxides, undercoordinated metal ions (e.g., Si^{4+}, Al^{3+}, Fe^{3+}) occurring on the top layer of oxide surfaces react with water molecules to form surface OH groups in an attempt to complete their coordination sphere. In the presence of water the surface of oxides, e.g., SiO_2, Fe_2O_3, Al_2O_3, TiO_2, are generally covered with surface hydroxyl groups (S-OH sites). For most of the oxides dissociative chemisorption of water molecules seems energetically favored [3, 4]. The various surface hydroxyls formed may structurally and chemically not be fully equivalent. Geometrical consideration and chemical measurements indicate an average surface density of 5 (typical range 2-12) hydroxyls per square nanometer of oxide surface [1, 3]. Surface hydroxyl groups of oxides can be removed by thermal treatment

in vacuum $O(MeOH)_2 \Leftrightarrow O(Me)_2O + H_2O$. These activated sites can be easily rehydrated by the adsorption of water, and farther water molecules can be adsorbed on the top of the already formed hydroxyls through the formation of hydrogen bonds [5]. The contact of magnetite nanoparticles with water molecules has been recently cleared up on the basis of our combined efforts of simulation and experiments [6]. The behavior of S-OH groups has been studied extensively and it is the subject of numerous reviews, e.g., [3, 4, 7]-[10].

Aluminum oxides and hydroxides chemisorb at least a monolayer of water when exposed to moisture [11]. Water is chemisorbed and the top layer of oxide ions is converted to hydroxyl ions, i.e., the reactive sites ($\equiv$Al-OH) on alumina surface.

Iron oxide particles with different crystal structures usually exist as colloidal particles (e.g., ferrihydrite $\sim$5-10 nm, goethite, hematite $\sim$10-50 nm). Under dry conditions surface Fe atoms may be coordinatively unsaturated [9]. In contact with water the iron atoms coordinate with water molecules which share their lone electron pairs with Fe. During adsorption, the water molecules usually dissociate resulting in a surface covered by hydroxyl groups coordinated to the underlying Fe atoms ($\equiv$Fe-OH sites). Hydroxylation of iron oxides is a fast reaction, it is followed by further adsorption of water molecules which hydrogen-bond to the surface OH groups as proved recently for magnetite, too [6]. The density of the most reactive singly coordinated groups is between 3 and 8 OH/nm^2.

In aqueous solutions the dissolution of oxides becomes often perceptible not only at extreme pH values. Comprehensive treatment of the dissolution of metal oxides has been given by Blesa et al. [12]. Solubility of different metal oxides and hydrolysis of the dissolved products are discussed in the book of Stumm and Morgan [4]. The activity of dissolved Al-species in equilibrium with gibbsite rises above 10^{-5} M below pH$\sim$4 and above pH$\sim$9. The sensitivity of ZnO and especially the amorphous $Zn(OH)_2(s)$ to pH is much pronounced than that of aluminum oxides. The concentration Zn species dissolved from the later increases above 10^{-4} M below pH$\sim$8.5 and above pH$\sim$11.5 [4]. In general, the solubility of iron(III) oxides (e.g., hematite, goethite) is low, the activity of dissolved iron(III) species remains below $\sim$10^{-5}$ M between pH$\sim$3 and $\sim$14 [9]. Reducing conditions enhance the solubility of iron(III) oxides. The presence of ligands such as chloride, fluoride, phosphate, citrate and several other anions that form soluble complexes with iron and aluminum, greatly promotes the dissolution of solid matrix.

2.2 Processes in aqueous phase

Several charged species are present even in the simplest aqueous solutions in contact with metal oxides. On the one hand charged species are released from solid phase due to hydrolysis, dissolution and dissociation processes discussed above. On the other hand indifferent electrolytes are present to provide constant ionic strength besides solute molecules, which are often capable to dissociate. The dissociation of small molecules in aque-

ous solutions, ionization processes of mono-, di- and oligoprotic acids and bases have been reviewed [14]. In aqueous systems a huge variety of different types of complexes has been identified depending on the chemical composition of solid and electrolyte solution. The complexation reactions in various aquatic systems are discussed in detail in the excellent book by Buffle [15]. Detailed chemical knowledge of the system is required to identify the probable equilibria. It may happen that anion of a background electrolyte such as Cl^-, PO_4^{3-} acts as a ligand related to the given metal ion (e.g., Zn^{2+}, Fe^{3+}, Al^{3+}) of the solute.

The formation of hydrolytic metal complexes such as $Al(OH)_3$, $Fe(OH)_3$, $Zn(OH)_2$ may lead to a significant decrease in solubility of metal ions over an appropriate range of pH. It has been proved that in the presence of solid particles, hydrolysable metal ions may precipitate on surface prior to bulk solution precipitation [4, 16].

Dissolution of sparingly soluble metal oxides in a multicomponent aqueous solution can be described by the set of the chemically probable heterogeneous and homogeneous reactions and the corresponding thermodynamic equilibrium constants, and by the mole balance equations for each component. Usually the set of coupled algebraic equation is too complicated to solve analytically, numerical procedures are required [17]. By now several computer programs are available that can calculate the equilibrium speciation, if thermodynamic equilibrium constants are known (e.g, MICROQL [18], MINTEQA [19]) or the set of experimental activity data can be fitted to obtain the equilibrium constants of probable reactions supposed in an appropriate chemical model (e.g., FITEQL [20]).

2.3 Adsorption of potential determining ions: surface charge formation

The hydroxyl groups on surface are bound chemically to the ions (e.g., Al^{3+}, Fe^{3+}, Ti^{4+}) in crystal lattice of oxides and hydroxides. These chemically reactive surface groups are exposed to an aqueous solution, surface becomes charged due to surface chemical reactions with H^+/OH^- ions [3, 4, 7, 21, 22]. The fact, that H^+ and OH^- ions are potential determining (p.d.) ions, however, has been the subject of special discussion since 1962 when de Bruyn assumed that for oxides. According to Lyklema [23] it is more appropriate to call H^+ and OH^- ions as charge-determining ions instead of p.d. ions, because these surfaces do not obey Nernst's law as analyzed for silicium-, aluminium- and iron-oxides by Hohl et al. [24]. The term charge-determining seems to be even worse than that substituted, since it would be nonsense, that the activity of H^+ and OH^- ions determines the surface charge density, as expected analogously to the definite dependence of surface potential on the activity of potential determining ions, since surface charge density changes characteristically in with varying ionic strength at constant activity of H^+ and OH^- ions.

Charge development on amphoteric surface sites (S-OH) could occur by direct proton transfer in surface protonation (S-OH + H^+ ⇔ S-OH$_2^+$)) and deprotonation (S-OH ⇔ S-O$^-$ + H^+) reactions [7, 14]. These can be considered as surface association-dissociation or interfacial adsorption-desorption processes. Charging of amphoteric oxide surface can be modeled with a simple one step protonation reaction (S-OH$^{-1/2}$ + H^+ ⇔ S-OH$_2^{+1/2}$) [25]. These interfacial equilibria can be characterized by equilibrium constants K or their negative logarithm pK, and so the above concepts are often differentiated as 2-pKs and 1-pK models [26].

When surface charge development occurs by direct proton transfer from aqueous phase, the surface charge density ($\sigma_{0,H}$) and surface potential (ψ_0) can be defined analogously to the Nernstian surfaces (F, R and T have the usual meaning):

$$\sigma_{0,H} = F(\Gamma_{H^+} - \Gamma_{OH^-}) \qquad (I)$$

$$\psi_0 = RT/F \ln[H^+]/[H^+]_{pzc}$$
$$= (RT/F)2.3(pH_{pzc} - pH) \qquad (II)$$

The surface charge density is experimentally accessible. The surface excess amounts (Γ_i) can be determined by means of adsorption measurements.

Ions in the solid-liquid interfacial layer are situated closer or further from the surface, depending on their size, charge, and ability to form chemical bonds with the surface sites. Ions which are constituents of the surface or have a particularly high affinity for surface sites are referred to as surface ions. This includes specifically adsorbed ions which can bind to the surface through covalent interactions in addition to the pure Coulombic contributions. The presence of these ions has a direct influence on the surface charge.

2.4 Distribution of indifferent ions at charged interface: charge neutralization

The ions are called as indifferent, which obey only electric constraints, i.e., either repulsion or attraction of Coulombic forces. The diffuse swarm of these ions is situated further from particle surface and they are electrostatically separated and disturbed by thermal motion. Although ions around particles are separated within a nanometer-scale distance, the surface charge must be balanced in the near-surface layer and the electrical neutrality condition in the electric double layer (EDL) must be satisfied. The *pure electrostatic approaches* based on the electrical neutrality constraint and the charge potential relationships derived from the Poisson-Boltzmann equation have been discussed previously [1]. It is worth recalling the charge potential relationship well-known as Gouy-Chapmann equation for the diffuse EDL:

$$\sigma_d = -(8\varepsilon_0\varepsilon_r kT)^{1/2}(n)^{1/2} \sinh(ze\psi_d/2kT) \qquad (i)$$

For small potentials ($ze\psi_d/2kT < 1$, $\psi_d <\sim 25$ mV), it is possible to expand sinh function ($\sinh x = x + x^3/3! \ldots$), and considering only the first term and the definition of κ parameter, the

following simplified equation can be deduced:

$$\sigma_d = -\varepsilon_0 \varepsilon_r \kappa \psi_d$$

Considering the charge neutralization constraint between the surface and diffuse layer charge densities ($\sigma_0 + \sigma_d = 0$) and supposing that $\psi_d = \psi_0$ at $x = 0$, we have

$$\sigma_0 = -\sigma_d = \varepsilon_0 \varepsilon_r \kappa \psi_0 \qquad \text{(ii)}$$

This simple equation obviously shows that any change in salt concentration is accompanied by change either in surface potential at constant σ_0, or in surface charge density at constant ψ_0. The surface charge density (σ_0) can be determined experimentally, for example from the surface excess concentration of p.d.-ions for conditionally charged solids like H^+/OH^- ions for oxides. However, the charge potential relation is a theoretical model-dependent function.

The Gouy-Chapmann model is based on only electrostatics (point charges in a dielectric continuum), it is proved to be a good approximation in general. Above equations can give the correct description of diffuse part of an electric double-layer further from the surface, but unrealistic values (very high surface potentials or extremely high local concentration of ions) close to the surface. Other equations from the adequate analytical solution of Poisson-Boltzmann equation known in basic literature [22, 27, 28], or even the numerical calculation can not overcome this inaccuracy. Corrections had to be introduced by which the finite volume of ions and the EDL structure at the closest distance to particle surface (i.e., chemical contributions in addition to electrostatic interaction) should be taken into consideration.

The *combined chemical and electrostatic models* have been developed to describe the distribution of charged species near particle surface. These are reviewed in several well-known writings [3, 4, 7, 14, 22, 27–29]. There are differences in the terminology and in the way these models are formulated, but they all have features in common: the reactions of surface groups are described by mass-action and material balance equations, and the surface potential is related to the surface charge by an electrostatic model [29].

Recently, the most often used models are called surface complexation models (SCMs). These combine the concept of coordination chemistry with those in electric double-layer theory. SCMs consider the surface charging (charge development on surface) and ion adsorption (interfacial distribution of ionic species) as surface complexation reactions. These processes are treated analogously to the homogeneous phase complexation equilibria described by mass action law in addition to the accounting the influence of electric potential developed in the interfacial reactions. The most common SC models are the constant capacitance, diffuse- and triple-layer models (CCM, DLM and TLM, respectively). A schematic representation of the surface complexation models is shown in Fig. 2. The distribution of charges in the electrified interface (top) and the potential de-

cay assumed in the given model in the near-surface region (middle) are shown. Some hypothetical surface species on oxides are represented (bottom), where surface sites (S-OH) are located at solid-liquid interface and the specifically adsorbed ions, hydrogen ions (H^+), cations or metal-ions (M^{m+}) and anions (A^{n-}) from the aqueous phase are presumed to form complexes with surface sites.
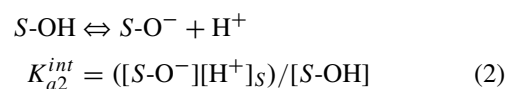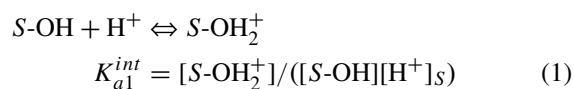
In all three models, charges associated with the surface are assumed to be balanced by counterion charges within a limited distance from surface. In the constant capacitance and diffuse-layer models all specifically adsorbed ions contribute to the surface charges (σ_0), it is balanced by the counterion charge. Charge potential relationship is linear ($\sigma_0 = \varepsilon_0 \varepsilon_r \kappa \psi_0$) in CCM. Counterion charges (σ_d) are situated in the diffuse part of EDL in DLM, and the electrical neutrality constraint is $\sigma_0 + \sigma_d = 0$. In the triple-layer model two near surface planes for adsorbing ions are distinguished. The surface species of specifically adsorbed H^+, OH^- ions pertain to the innermost part and it is characterized by charges σ_0, and the outer plane has charges σ_β resulting from the adsorption of other ions. Since electric field extending away from surface is the direct result of the surface complexation reactions of specific ions in the near surface region, the specifically adsorbed ions also govern the counterion distribution in the diffuse layer. The charge balance of three layers can be written as $\sigma_0 + \sigma_\beta + \sigma_d = 0$.

The activity of ions near the surface, $[X^z]_S$, are influenced by the electrostatic field arising from the surface charge. It is distinguished from that in the bulk solution, $[X^z]$, because the difference in electrical potential at distance x from the surface, relative to that in the bulk solution, ψ_x, applying the Boltzmann distribution is

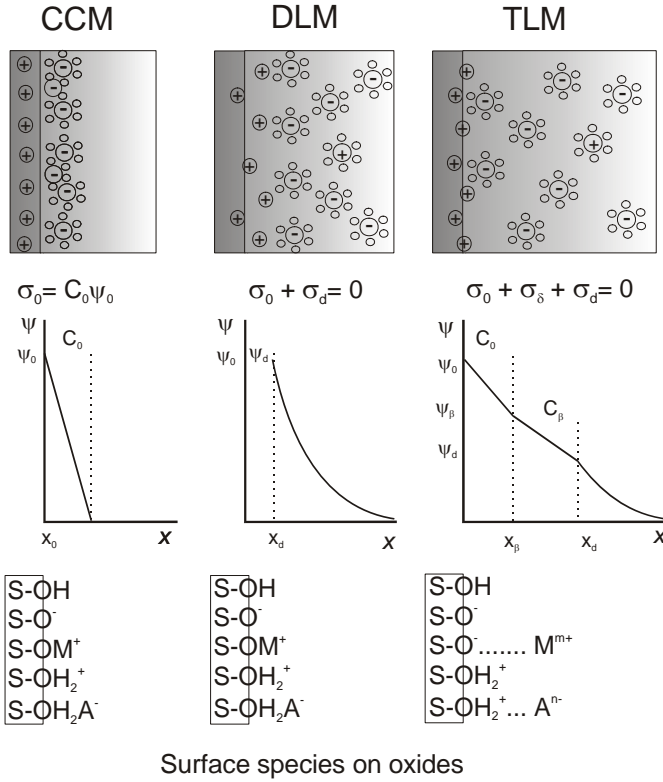$$[X^z]_S = [X^z] \exp(-ez\psi_x/kT) \qquad \text{(iii)}$$

where $ez\psi_x$ is the electric potential energy (or electrical work in moving the ions from bulk to distance x), z is the charge of ion X, e is the electron charge, kT is the thermal energy, k is the Boltzmann constant and T is the temperature.

Surface complexation reactions are assumed on surface sites, S-OH. The total site density (N_S, mol/m^2) has to be defined for the given system. In the constant capacitance and diffuse layer model all surface species are supposed to be inner-sphere complexes, while in the triple layer model both inner- and outer-sphere complexes are assumed. The following protonation and deprotonation equilibria can represent the charge formation on surface site, S-OH:

$$S\text{-OH} + H^+ \Leftrightarrow S\text{-OH}_2^+$$
$$K_{a1}^{int} = [S\text{-OH}_2^+]/([S\text{-OH}][H^+]_S) \qquad (1)$$
$$S\text{-OH} \Leftrightarrow S\text{-O}^- + H^+$$
$$K_{a2}^{int} = ([S\text{-O}^-][H^+]_S)/[S\text{-OH}] \qquad (2)$$

where K_{a1}^{int} and K_{a2}^{int} are the invariant, intrinsic equilibrium constants; brackets mean the activity of species. The surface

Surface complexation models

CCM   DLM   TLM

$$\sigma_0 = C_0\psi_0 \qquad \sigma_0 + \sigma_d = 0 \qquad \sigma_0 + \sigma_\delta + \sigma_d = 0$$

S-OH	S-OH	S-OH
S-O⁻	S-O⁻	S-O⁻
S-OM⁺	S-OM⁺	S-O⁻ .... M^{m+}
S-OH₂⁺	S-OH₂⁺	S-OH₂⁺
S-OH₂A⁻	S-OH₂A⁻	S-OH₂⁺... A^{n−}

Surface species on oxides

Fig. 2. Schematic representation of SCMs: CCM, DLM and TLM; charge distribution (top) and potential decay (middle) within a nanometer-scale distance and surface species on oxides (bottom).
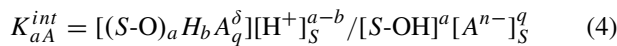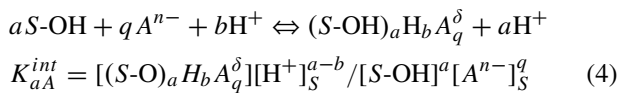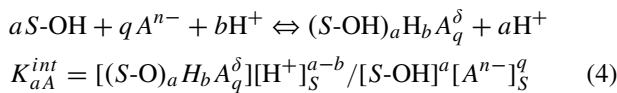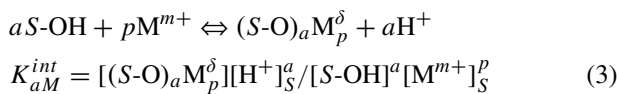
species, S-OH, S-OH$_2^+$, S-O$^-$, are assumed to have activity coefficients equal to unity. However, the activity of surface hydrogen ions, [H$^+$]$_S$, has to be corrected for the energy expended in moving them to the charged surface (at distance $x = 0$) where reaction occurs. Expressing [H$^+$]$_S$ in term of the bulk solution hydrogen ion activity, [H$^+$], is

$$[\text{H}^+]_S = [\text{H}^+]\exp(-e\psi_0/kT) \qquad (iv)$$

The conventional mass action quotients without electric potential variable for these equilibria are not constants, often called as apparent equilibrium constants, K^{app} and K^{app}, or operational reaction quotients, Q_{a1} and Q_{a2}. Intrinsic equilibrium constants for surface charge formation can be determined by means of an extrapolation at zero electric potential [3, 4, 15]:

$$\lim_{\psi_0 \to 0} \log K^{app} = \log K^{int}$$

Surface complexation reaction for multivalent ions (M^{m+} and A^{n-}) can be written

$$aS\text{-OH} + p\text{M}^{m+} \Leftrightarrow (S\text{-O})_a\text{M}_p^\delta + a\text{H}^+$$
$$K_{aM}^{int} = [(S\text{-O})_a\text{M}_p^\delta][\text{H}^+]_S^a/[S\text{-OH}]^a[\text{M}^{m+}]_S^p \qquad (3)$$
$$aS\text{-OH} + q\text{A}^{n-} + b\text{H}^+ \Leftrightarrow (S\text{-OH})_a\text{H}_b\text{A}_q^\delta + a\text{H}^+$$
$$K_{aA}^{int} = [(S\text{-O})_a\text{H}_b\text{A}_q^\delta][\text{H}^+]_S^{a-b}/[S\text{-OH}]^a[\text{A}^{n-}]_S^q \qquad (4)$$

The distribution of ions H$^+$, M^{m+} and A^{n-} between the surface layer and bulk solution is governed by the electrostatic field,

and Eqs. (iii) and (iv) can be applied by substituting surface potential, ψ_0, in all cases, if CCM and DLM models are applied, since only inner-sphere complex formation is assumed and all the ions are assigned to near the surface; while potential ψ_β is substituted in Eq. (iii) for distribution of ions M^{m+} and A^{n-} when TLM model is chosen, since proton transfer processes are assigned to the surface and complexation of other ions, which form outer-sphere complexes, to the β-plane in the TLM model.

The charge potential relationship can be given by appropriate form of Eqs (i) and (ii)

$$DLM \quad \sigma_0 = (8\varepsilon_0\varepsilon_r kT)^{1/2}(n^0)^{1/2}\sinh(ze\psi_0/2kT)$$
$$CCM \quad \sigma_0 = C_0\psi_0$$
$$TLM \quad \sigma_0 = C_0(\psi_0 - \psi_\beta)$$
$$\sigma_\beta = C_0(\psi_\beta - \psi_0) + C_\beta(\psi_\beta - \psi_d)$$
$$\sigma_d = C_\beta(\psi_d - \psi_\beta)$$
$$\sigma_d = -(8\varepsilon_0\varepsilon_r kT)^{1/2}(n)^{1/2}\sinh(ze\psi_d/2kT)$$

where σ_0, σ_β and σ_d are the total charges associated with the inner, outer and diffuse planes, C_0 and C_β are the capacitances associated with the zones between the inner and outer, and outer and diffuse planes, respectively, ψ_0, ψ_β and ψ_d are the electrostatic potentials at the surface, inner and outer planes, respectively. It should be noted that application of these models needs an appropriate choice of units of physical quantities.

Application of the surface complexation models for the description of a given system presumes first the definition of the assumed chemical processes, then determination of intrinsic equilibrium constants. Previously different graphical extrapolation methods [3, 4, 15, 22] were used, lately the FITEQL [20] program provides an elegant numerical way to calculate the intrinsic constants together with the possible choice of different complexation models.

3 Experimental

Potentiometric acid-base titration of oxides provides a direct measure of net proton surface charge density [22, 30], if the ions of background electrolyte have no specific affinity for the surface (called as indifferent electrolyte), and the total acid or base consumption results in surface charge formation, as well as no any other acid-base reactions, like hydrolysis, dissolution, take place.

The pH-dependent surface charge was determined by potentiometric acid-base titration under CO$_2$-free atmosphere. Solid samples (0.3 to 1 g) of the purified metal oxides were titrated. An indifferent electrolyte (NaCl, KCl, KNO$_3$) was used to maintain a constant ionic strength ranging between 0.001 and 1 M. Before titration, the suspensions or solutions were stirred and bubbled by purified nitrogen for 15 min. Equilibrium titration was performed in a self-developed titration system (GIMET1) consisting of two Dosimat 665 burettes (Metrohm), a nitrogen bubbling, a magnetic stirrer and a high performance potentiometer. The course of the titration (amount and frequency

of titrant, bubbling, stirring, millivolt measurement) was controlled by an IBM PS/1 computer using AUTOTITR software. The pH-measuring Radelkis OP-0808P (Hungary) combination glass electrode was calibrated using three buffer solutions (Radelkis, Hungary) to check the Nernstian response. The evaluation of titration data was based on the calculation of the material balance for H^+/OH^- ions. The measuring system had to be calibrated for H^+/OH^- ion concentration, which in turn was put into the material balance equations. The experimental activity coefficients of H^+/OH^- ions were determined from the background electrolyte titration at the each ionic strength. The H^+/OH^- concentration was calculated knowing the concentration of acid and base titrants, the volume of portions and the dilutions, and their activities were calculated from the measured pH and the ionization constant of water. If the response of glass electrode is perfect, the activity vs. concentration plots give straight lines, and their slopes provide the values of experimental activity coefficient at different electrolyte concentrations.

The net proton surface excess amount ($\Delta n^\sigma = n^\sigma_{H^+} - n^\sigma_{OH^-}$) is defined as the difference between H^+ ($n^\sigma_{H^+}$) and OH^- ($n^\sigma_{OH^-}$) surface excess amounts related to the unit mass of solid. The surface excess amount of a solute i (Γ_i) can be determined experimentally from the initial ($c_{i,0}$) and the equilibrium concentration ($c_{i,e}$) of the solute ($n^\sigma_i = V(c_{i,0} - c_{i,e})/m$, where V is the liquid phase volume and m is the mass of the adsorbent; $\Gamma_i = n^\sigma_i/a^s$, where a^s is the specific surface area of the adsorbent) for adsorption from dilute solutions [27]. The values of excess $n^\sigma_{H^+}$ or $n^\sigma_{OH^-}$ were calculated at each point of titration from the initial and the equilibrium concentrations of the H^+ and OH^- ions using the actual activity coefficient from the slope of H^+/OH^- activity vs. concentration straight lines for background electrolyte titration. Roughly tenth part of the total active site density calculated from crystallographic data can be titrated, or with other words only 10% of surface hydroxyls can become charged.

Since this method is based on the determination of the change in H^+/OH^- concentration in the liquid phase due to interfacial proton transfer processes, any acid/base impurities of the titrated sample and its dissolution at extreme pHs will interfere with the surface charge density, as showed for magnetite and alumina before [31, 32], and so careful sample preparation is required. In the case of magnetite and hematite, the stock suspension was stored in 0.001 M HCl, so its medium contained excess H^+ ions. Therefore the equilibrium supernatant obtained by centrifugation at 13000 RPM for 2 hours was also titrated in parallel with suspensions.

4 Results and Discussion

It has to note first that the complex aspect of aqueous dispersions shown in Fig. 1 has not been widely accepted. Although it is evident that the processes depending on the chemical background do take place independently of our knowledge, I have hardly found a systematic analysis of all probable simultaneous

equilibria in the relevant literature. In the most cases the solution condition such as pH dependent dissolution of solid phase, the surface precipitation and the speciation in aqueous phase are omitted in the evaluations either without mentioning them or with reference to some reasoning.

The evaluation of the experimental data from acid-base titration of amphoteric solid material demands cautious work. The different approaches are accepted in the literature and summarized perhaps in the most comprehensive way in the book of Kosmulski [26]. With respect to the solution chemistry, the experimental data of colloid titration are significantly less accurate and reproducible than that in homogeneous systems. The situation at the electrified interface is more complicated. Other acid or base consuming reactions (e.g. presence of acid/base impurities, dissolution of solid at lower or higher pHs) can take place in parallel with the surface charging processes, which cannot be separated experimentally as analyzed in [1]. However, excluding all of these the net proton surface excess amount related to the unit mass of solid can be calculated directly and plotted as a function of pH. In the case of magnetite and hematite, since the stock suspension was stored in 0.001 M HCl, both the surface and the medium contained excess H^+ ions in an exactly unknown amount. The double calibration of our titration system for the pH and the H^+/OH^- concentration allowed us to correct the measured net proton consumption of iron oxide suspensions. On the one hand the H^+ concentration of the equilibrium supernatant was measured and proved to be independent of NaCl concentration over the range of pH 3 to 9, so its additive correction became possible. On the other hand the surface excess H^+ concentration in the initial state at pH~3 and 0.001 M ionic strength was estimated and subtracted from the calculated material balance of H^+/OH^- ions during titration. The Al_2O_3 (Aluminium oxide C) and TiO_2 (Titanium dioxide P25) of Degussa were produced by flame hydrolysis of $AlCl_3$ and $TiCl_4$, and the samples always contain some non-hydrolysed residual of metal chlorides. Therefore these samples have to be carefully purified by either heating alumina up to 1000 ^{o}C [32] or exhaustive washing titania with water before titration.

The surface charging of oxide particles varies characteristically with pH and ionic strength as the effects of specific and indifferent ions, respectively. It is worth showing first, the simple cases of the surface-charge titration of purified oxide samples (Fig. 3). Experimental curves of potentiometric acid-base titrations representing the net proton surface excess amount (either $\Delta n^\sigma = n^\sigma_{H^+} - n^\sigma_{OH^-}$ or $\Delta\Gamma_{H,OH} = \Gamma_{H^+} - \Gamma_{OH^-}$) as a function of pH often called as charge potential curves, since the net proton surface excess is proportional to the surface charge density (σ_0 given in Eq. (I)), while pH is to the surface potential (ψ_0 given in Eq. (II)). These are determined at several concentrations of indifferent electrolyte and show the characteristic opening feature with increasing ionic strength (I), which is resulted from the Eq. (ii) $\sigma_0 = -\sigma_d = \varepsilon_0\varepsilon_r\kappa\psi_0$ considering that κ increases with I and so σ_0 does in the same way, since ψ_0 should
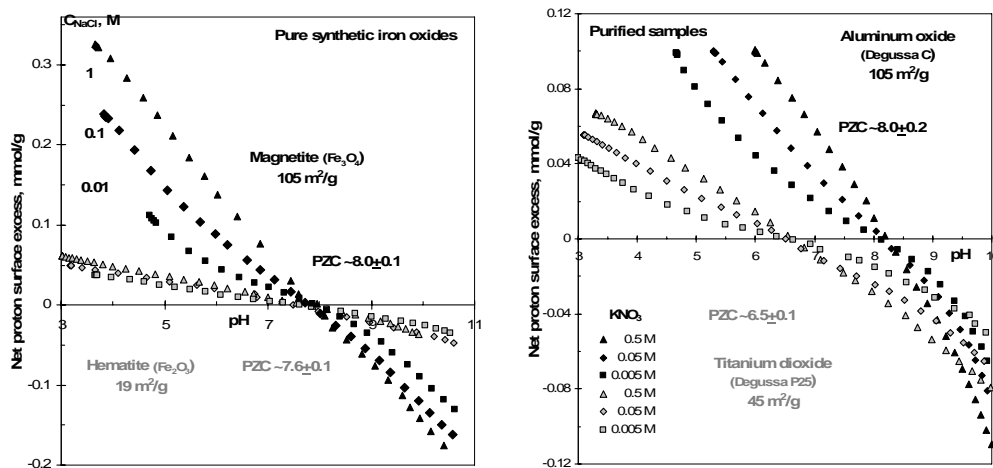
Fig. 3. Experimental charge potential curves of purified metal oxides dispersed in the solutions of indifferent electrolytes, the pH values of common intersection points are identified as points of zero charge (PZC); oxide samples have different compositions and specific surface areas.

be constant at constant pH. Charge potential curves can intersect at a common pH. It can be called as common intersection point (c.i.p.) [23]. If the c.i.p. of $\sigma_{0,H}$ (or $\Delta\Gamma_{H,OH}$) versus pH curves is sharp and coincides with the $\sigma_{0,H} = 0$ (where $\Gamma_{H+} = \Gamma_{OH-}$), surface charge state, this unique pH is then identified as the point of zero charge, PZC as given in Figs. 3a,b. This occurs only in the case of oxides under ideal conditions [23]. The point of zero charge is a characteristic of the given surface in aqueous medium, it is the reference point for surface charging [27]. The reliable experimental data of PZC, sometimes called as pristine point of zero charge, (PPZC) [23, 27], for several oxides are collected in literature [7, 9, 27]. The biggest collection of PZC values can be found in the book of Kosmulski [26].

The pH- and ionic strength-dependent surface charge formation process can be described by various model approximations, the most widely accepted models are the site-binding electrostatic or surface complexation models (SCMs) models (e.g. James and Parks [7]; Hunter [28]; Kosmulski [26]; Borkovec et al. [14]). The experimental data of purified alumina and magnetite titration were evaluated using a numerical data-fitting program FITEQL [20]. The choice of different surface complexation (constant capacitance (CC), diffuse layer (DL), Stern and triple layer (TL)) models is optional. The measured data of both aluminium and iron oxide titration might be well fitted by choosing any SC model. An example for the quality of the fitting of curves optimized by FITEQL using CC approach and the experimental points calculated on the basis of material balance of added H^+/OH^- is shown in Fig. 4. The experimental points are fitted quite well even using the simplest CC approach of SCMs. Detailed comparison of results from fitting different SCMs has been published previously [32]. The pH of the PZC can be calculated according to the relation $PZC = 0.5(\log K_{a,1}^{int} - \log K_{a,2}^{int})$ [7, 9, 23] from the equilibrium constants given in the legend of Fig. 4. These are PZC_{calc} 8.1± 0.1 and 7.9 ± 0.2 for alumina and magnetite, respectively; both correlate well with the experimental PZC observed as c.i.p

of charge potential curves. The values in literature [26] agree more or less well with our model calculation. It should be noted that the experimental conditions and quality of aluminium and iron oxide samples are always more or less different, and so the variables (specific surface area, ionic strength, etc.) and the calculated $\log K$ values are also somewhat different. The experimental net proton consumption vs. pH functions of the original and purified alumina and titania samples are obviously different as shown in Fig. 5. One of the conspicuous features is the difference in the initial pH of suspensions. In the suspensions of the purified oxide samples, the pH is almost independent of ionic strength, and it is close to their PZC. However, the pH in the suspensions of original samples significantly increases with increasing salt concentration, since the increasing concentration of chloride ions in the equilibrium liquid phase hinders the propagation of the hydrolysis of metal chlorides:

$$AlCl_3 + 3H_2O \leftrightarrows Al(OH)_3 + 3H^+ + 3Cl^-$$

$$TiCl_4 + 4H_2O \leftrightarrows Ti(OH)_4 + 4H^+ + 4Cl^-$$
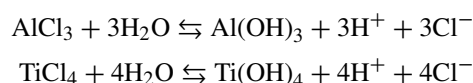
The common intersection points of curves measured at different ionic strengths are significantly different for original and purified samples. These c.i.p. points can be assigned as the point of zero salt effect (PZSE at which $(\delta\sigma_{0,H}/\delta I)_{pH}$ is zero) introduced by Sposito [22, 30] shift up after removal of metal chloride contamination showing the absence of base consuming hydrolysis product (H^+) in both cases. The estimated amounts of H^+ released from the original samples are 0.083 and 0.022 mmol/g (-Δq at the c.i.p. of alumina and titania, respectively) are in good harmony with the maximum amount of Cl^- measured directly in the samples (0.081 and 0.028 mmol/g for alumina and titania, respectively).

Although the pHs of c.i.p. points belonging to the original contaminated samples hardly differ from the PZC values of purified samples measured under ideal condition, a simple additive correction of the experimental proton consumption curves, i.e. an up/down shift of $\Delta q_{H,OH} = 0$ or $\sigma_H = 0$ line done often in
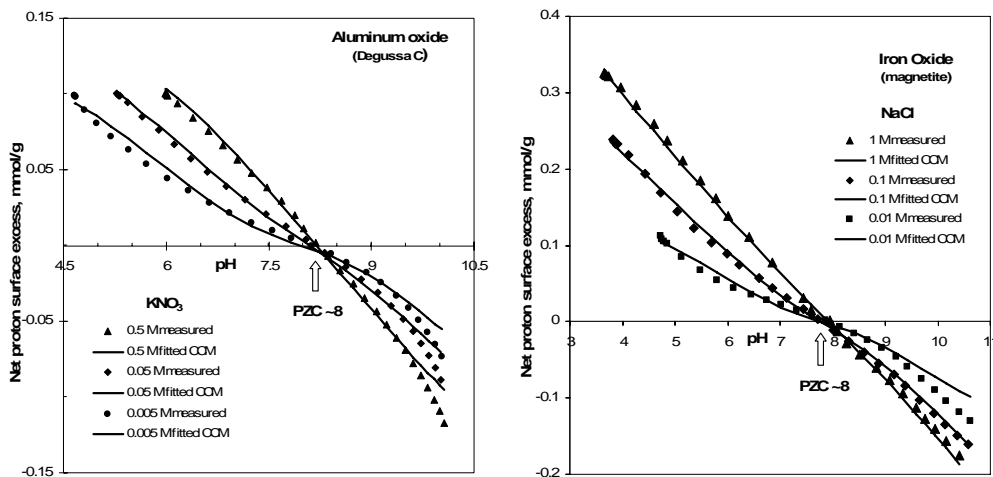
Fig. 4. Experimental points of net proton surface excess amounts for purified δ-Al$_2$O$_3$ (left) and Fe$_3$O$_4$ magnetite (right) as a function of pH at different concentrations of indifferent electrolytes (KNO$_3$ and NaCl, respectively) at room temperature. The points were calculated from the material balance of H$^+$/OH$^-$ in the course of equilibrium acid-base titration. The continuous lines were numerically fitted using FITEQL [20] (constant capacity model for alumina and magnetite using capacities C=1.2 and 1.6 F/m^2, respectively). The calculated equilibrium constants are $\log K_{a,1}^{int}$=7.1±0.5 and $\log K_{a,2}^{int}$=-9.1±0.3 for alumina [32], and $\log K_{a,1}^{int}$=6.6±0.1 and $\log K_{a,2}^{int}$= -9.1±0.1 for magnetite [31].
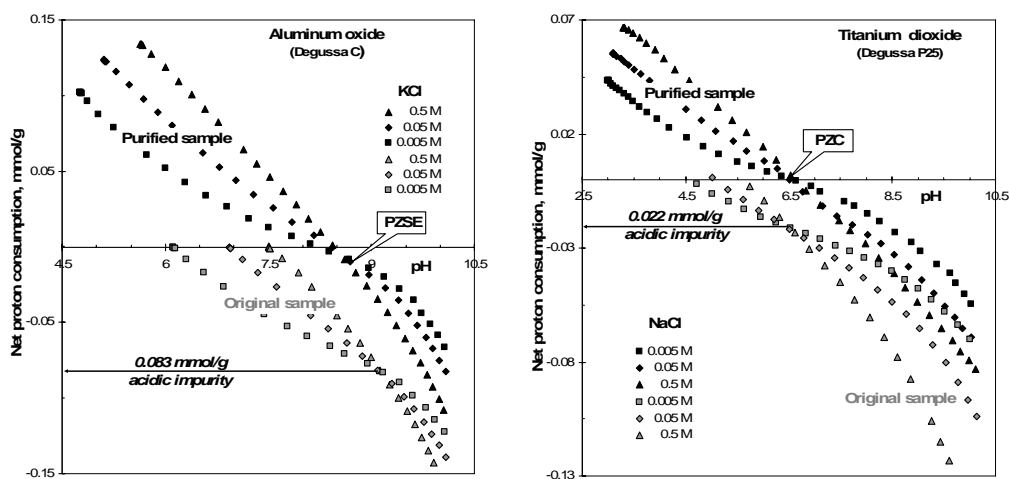

Fig. 5. The effect of acidic impurity on experimental points of alumina and titania samples produced by flame hydrolysis of aluminum and titanium chlorides. The points were calculated from the material balance of H$^+$/OH$^-$ in the course of equilibrium acid-base titration.

the literature [26], can not be a correct way of experimental data evaluation.

The effect of dissolution is often neglected in the evaluation of charge potential curves. Dissolution of aluminium oxide in both acidic and alkaline solutions and its dependence of the crystal structure is well-known [33]. Below pH~4 and above pH~10, the dissolution of this amphoteric solid becomes observable; therefore, the interfacial charging is often studied within these pHs [34, 35]. Study on dissolution kinetics of aluminum oxide [36] shows that the dissolution rate considerably depends on the pH of aqueous solution, a minimum was observed near neutral pH; the dissolution rate increased with decreasing pH below pH 6 and (even more strongly) with increasing pH above pH 7.5. The net dissolution rate was in order of magnitude 1 10^{-8} mol/ h m^2 at pH 4 and 9. Considering the high specific surface area of alumina measured in general by means of potentiomet-

ric acid-base titration method and the endeavor of experimenters to reach equilibrium state of surface-charging by increasing the time of titration, it is highly probable to suppose that the experimental charge potential curves are disturbed by the H$^+$/OH$^-$ consumption from dissolution, even those which were measured over the likely dissolution-free pH range. In some works, the possibility of alumina dissolution is excluded with reference to the chemical equilibrium calculation [34] or it is not mentioned [37]-[39] at all. Fitting of experimental surface-charging curves led to more and more complicated theoretical approaches with increasing number of layers for charge-compensating ions in the surface complexation models (diffuse double-, triple-, and four-layer models [38, 39]) and with introducing surface site heterogeneity parameters. The heterogeneity of proton binding sites at oxide-solution interface is studied theoretically [40]-[42] and both theoretically and experimentally [5, 34, 37]-[39, 43].
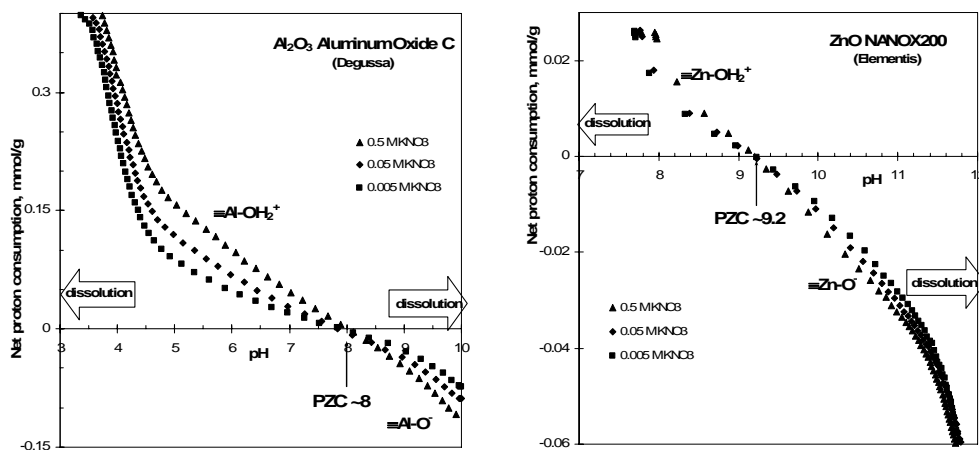
Fig. 6. Experimental net proton consumption curves for purified δ-Al$_2$O$_3$ (left) and ZnO (right) nanoparticles dispersed in KNO$_3$ solutions at room temperature. The points were calculated from the data measured in the direction of decreasing and increasing pH of equilibrium titration with acid and base solutions for Al$_2$O$_3$ (left) and ZnO (right), respectively.

Based on potentiometric titration performed over a broad range of pH's (3-11), affinity distributions for four different surface sites were calculated with the aim of studying the heterogeneity of acid-base properties at aluminum oxide-solution interface [43]. These authors neglected both the electrostatic effect and the dissolution of alumina. Although alumina dissolution under the given experimental conditions was checked and its contribution to the total H$^+$/OH$^-$ consumption seemed to be not significant, the experimental fact that the measured proton adsorption isotherms became independent of ionic strength below pH~4 and above pH~10 refers that other reactions taking place in parallel with surface charging, as seen obviously in the acidic region of alumina titration (Fig. 6 left) in the present case, too. Asymmetric proton-binding curves were measured [34] over the pH range 5-11. The unusually high OH$^-$ excess in alkaline region was modeled by assuming the penetration of electrolyte ions into the surface, whereas the probability of OH$^-$ consumption due to dissolution was limited to some percents [34]. We analyzed and modelled the dissolution problem in detail before [1, 32]. The dissolution of alumina and the assumed speciation of hydrolysis products were proved experimentally by means of measuring the total aluminium concentration in equilibrium supernatants of alumina suspensions over the range of pH relevant to the titration by an independent method. It has been stated that only the independent experimental evidence(s) can support effectively the model assumption(s).

Even the shape of net proton consumption curves for ZnO (Fig. 6 right) indicates the dissolution of crystals especially in the alkaline region. This was confirmed by the good coincidence of dissolution limits below pH~8 and above pH~11 with the pH values given in literature [4].

It has to be stated that the definite change in the shape of charge-potential curves, when their ionic strength dependence does not exist any more is indicative of the acid or base consumption reactions anything else than surface charge formation. The most relevant reaction is the acid/base dissolution of amphoteric solids like metal oxides. The dissolution rate of metal oxides, however, strongly depends on the pH of aqueous solution and the specific surface area of solid; its interference first becomes obvious in the equilibrium potentiometric titration preformed during long time and only at low and high pH's, and especially in the case of nanoparticles having high specific surface areas. The goodness of fit between the experimental points and the calculated curves from a model based on even a sophisticated, advanced theory [34] does not prove the reality of any theoretical model, the assumed structure of surface layer and the presumed interfacial reactions. Any model assumption has to be supported by independent experimental facts (e.g., surface spectroscopy, analysis of equilibrium bulk phase) to prove its reality.

5 Conclusion

The surface charge formation of metal oxides can be characterized by acid/base titration; however, other processes such as hydration of surface, dissociation of surface sites, dissolution of solid matrix at aqueous interface, then hydrolysis of dissolved ions in aqueous phase take place simultaneously even in the simplest case, which are often not considered. The specific adsorption of H$^+$/OH$^-$ on surface hydroxyl groups, i.e., protonation and deprotonation reactions, in the presence of indifferent electrolytes results in pH-dependent charges on the surface of metal oxides. The charge potential curves calculated from the measured data can easily fit by SCMs assuming several parameters which can be varied to fit experiment; and so good fitting may be achieved without giving any relevant insight into the processes occurring. A detailed chemical knowledge of the system is required in order to verify the assumptions involved in the model, otherwise the application of SCMs becomes a meaningless exercise of curve fitting. From a general standpoint, the critical assumptions of the surface complexation models are the relevant specific surface area, the quality and quantity of active sites involved in the interfacial processes, and the nature of the surface complex(es) formed (quality and strength of chemical bonds on

surface sites). The definite advantage of SCM is that it can be simply combined with the aqueous bulk equilibria such as speciation of hydrolyzing metal ions, complex formation.

References

1 **Tombácz E**, *Adsorption from electrolyte solutions*, Adsorption: Theory, Modeling, and Analysis (Tóth J, ed.), Marcel Dekker, New York, 2002, pp. 711-742.

2 **Wensink E J W, Hoffmann A C, Apol M E F, Berendsen H J C**, *Properties of Adsorbed Water Layers and the Effect of Adsorbed Layers on Interparticle Forces by Liquid Bridging*, Langmuir **16** (2000), 7392, DOI 10.1021/la000009e.

3 **Stumm W**, *Chemistry of the Solid-Water Interface, Processes at the Mineral-Water and Particle-Water Interface in Natural Systems*, Wiley, New York, 1992.

4 **Stumm W, Morgan J J**, *Aquatic Chemistry, Chemical Equilibria and Rates in Natural Waters*, Wiley, New York, 1996. 3rd Edition.

5 **Rudzinski W, Charmas R, Borowiecki T**, *Adsorption on New and Modified Inorganic Sorbents Studies in Surface Science and Catalysis*.

6 **Tombácz E, Hajdú A, Illés E, László K, Garberoglioc G, Jedlovszky P**, *Water in Contact with Magnetite Nanoparticles, as Seen from Experiments and Computer Simulations*, Langmuir **25** (2009), 13007, DOI 10.1021/la901875f.

7 **James R O, Parks G A**, Surface and Colloid Science (Matijevic E, ed.), Vol. 12, Plenum, New York, 1982, pp. 119-216.

8 **Sposito G. (ed.)**, *The Environmental Chemistry of Aluminum*, CRC Press, Boca Raton, 1989.

9 **Cornell R M, Schwertmann U**, *The Iron Oxides, Structure, Properties, Reactions, Occurrence and Uses*, VCH, Weinheim, 1996.

10 **Iler R K**, *The Colloid Chemistry of Silica and Silicates*, Cornell Univ. Press, Ithaca, New York, 1955.

11 **Hemingway B S, Sposito G**, The Environmental Chemistry of Aluminum (Sposito G, ed.), CRC Press, Boca Raton, 1989, pp. 55-85.

12 **Blesa M, Morando B J, Regazzoni A E**, *Dissolution of Metal Oxides*, CRC Press, Boca Raton. FL. 1994.

13 **Davis J A, Hem J D**, *The Environmental Chemistry of Aluminum* (Sposito G, ed.), CRC Press, Boca Raton, 1989.

14 **Borkovec M, Jönsson B, Koper G J M**, *Ionization processes and proton binding in polytropic systems: small molecules, proteins, interfaces and polyelectrolytes*, Surface and Colloid Science Vol. 16 (E Matijevic E, ed.), Kluwer Academic/Plenum Press, 2001, pp. 99-339.

15 **Buffle J**, *Complexation Reactions in Aquatic systems: An analytical Approach*, Ellis Horwood Ltd., Chichester, 1988.

16 **Fendorf S E, Sparks C L**, *Surface precipitation reactions on oxide surfaces*, J. Colloid Interface Sci. **148** (1992), 295, DOI 10.1016/0021-9797(92)90141-8.

17 **Sposito G**, *The Thermodynamics of Soil Solutions*, Clarendon Press, Oxford, 1981.

18 **Coves J, Sposito G**, *MICROQL-UCR: A surface chemical adaptation of the speciation program MICROQL*, University of California, Riverside, CA, USA, 1989.

19 **Allison J D, Brown D S, Novo-Dradac K J**, *MINTEQA2/PRODEFA2, v.3.0.*, U.S. EPA, Athens, GA, USA, 1991.

20 **Herbelin A L, Westall J C**, *FITEQL v.3.2*, Oregon State University, Corvallis, OR, USA, 1996.

21 **Koopal L K**, *Studies in Surface Science and Catalysis Vol. 99* (Dabrowski A, V A Tertykh A, eds.), Elsevier, Amsterdam, 1996.

22 **Sposito G**, *The Surface Chemistry of Soils*, Oxford University Press, New York, 1984.

23 **Lyklema J**, *Nomenclature, symbols, definitions and measurements for electrified interfaces in aqueous dispersions of solids*, Pure Appl. Chem. **63** (1991), 895, DOI 10.1351/pac199163060895. (Recommendations 1991).

24 **Hohl H, Sing J, Stumm W**, *Particulates in Water* (Kavanaugh M C, Leckie J O, eds.), 1980. ACS 189.

25 **Hiemstra T van Riemsdijk W H**, *Physical chemical interpretation of primary charging behaviour of metal (hydr) oxides*, Colloids Surfaces **59** (1991), 7, DOI 10.1016/0166-6622(91)80233-E.

26 **Kosmulski M**, *Chemical properties of material surfaces*, Marcel Dekker, New York, 2001.

27 **Lyklema J**, *Fundamentals of Interface and Colloid Science, Vol. I and II, Vol. I. Fundamentals, Vol. II: Solid-Liquid Interfaces*, Academic Press, London, 1991.

28 **Hunter R J**, *Foundations of Colloid Science, Vol. I and II*, Clarendon Press, Oxford, 1989.

29 **Haworth A**, *A review of the modelling of sorption from aqueous solution*, Adv. Colloid Interface Sci. **32** (1990), 43, DOI 10.1016/0001-8686(90)80011-N.

30 **Sposito G**, *Environmental Particles Vol.1* (Buffle J, van Leeuwen H P, eds.), Lewis, Boca Raton, 1992.

31 **Tombácz E, Illés E, Majzik A, Hajdú A, Rideg N, Szekeres M**, *Ageing in the Inorganic Nanoworld: Example of Magnetite Nanoparticles in Aqueous Medium*, Croatica Chemica Acta **80** (2007), 503-515.

32 **Tombácz E, Szekeres M**, *Interfacial Acid-Base Reactions of Aluminum Oxide Dispersed in Aqueous Electrolyte Solutions. 1. Potentiometric Study on the Effect of Impurity and Dissolution of Solid Phase*, Langmuir **17** (2001), 1411-1419, DOI 10.1021/la001322j.

33 **Lindsay W L, Walthall P M**, *The Environmental Chemistry of Aluminum* (Sposito G, ed.), CRC Press, Boca Raton, Florida, 1989.

34 **Hiemstra T, Yong H, Van Riemsdijk W H**, *Interfacial Charging Phenomena of Aluminum (Hydr)oxides*, Langmuir **15** (1999), 5942, DOI 10.1021/la981301d.

35 **Wood R, Fornasiero D, Ralston J**, *Electrochemistry of the boehmite—water interface*, Colloid Surfaces **51** (1990), 389, DOI 10.1016/0166-6622(90)80154-V.

36 **Kraemer S M, Chiu V Q, Hering J G**, *Influence of pH and Competitive Adsorption on the Kinetics of Ligand-Promoted Dissolution of Aluminum Oxide*, Environ. Sci. Technol. **32** (1998), 2876, DOI 10.1021/es980253g.

37 **Rudzinski W, Charmas R, Partyka S, Thomas F, Bottero J Y**, *On the nature of the energetic surface heterogeneity in ion adsorption at a water oxide interface: the behavior of potentiometric, electrokinetic, and radiometric data*, Langmuir **8** (1992), 1154, DOI 10.1021/la00040a023.

38 **Charmas R, Piasecki W**, *Four-Layer Complexation Model for Ion Adsorption at electrolyte/Oxide Interface: Interrelations of Model Parameters*, Langmuir **12** (1996), 5458, DOI 10.1021/la960234p.

39 **Charmas R**, *Four-Layer Complexation Model for Ion Adsorption at Energetically Heterogeneous Metal Oxide/Electrolyte Interfaces*, Langmuir **15** (1999), 5635, DOI 10.1021/la980880j.

40 **Cernik M, Borkovec M, Westall J C**, *Affinity Distribution Description of Competitive Ion Binding to Heterogeneous Materials*, Langmuir **12** (1996), 6127, DOI 10.1021/la960008f.

41 **Borkovec M**, *Origin of 1-pK and 2-pK Models for Ionizable Water-Solid Interfaces*, Langmuir **13** (1997), 2608, DOI 10.1021/la9621325.

42 **Rustad J R, Wasserman E, Felmy A R, Wilke C**, *Molecular Dynamics Study of Proton Binding to Silica Surfaces*, J. Colloid Interface Sci. **198** (1998), 119.

43 **Contescu C, Jagiello J, Schwarz J A**, *Heterogeneity of proton binding sites at the oxide/solution interface*, Langmuir **9** (1993), 1754, DOI 10.1021/la00031a024.